CILAMCE 2017
Florianópolis - Santa Catarina - Brazil

COMPARATIVE ANALYSIS OF FLUID TOPOLOGY OPTIMIZATION ALGORITHMS BASED ON ADJOINT METHODS

Eduardo Tadashi Katsuno

eduardo.katsuno@usp.br

Escola Politécnica da USP

Av. Prof. Mello Moraes, 2231, 05508-030, Sao Paulo, SP, Brazil

Carlos Massaiti Okubo Júnior

cmojr1@gmail.com

Escola Politécnica da USP

Av. Prof. Mello Moraes, 2231, 05508-030, Sao Paulo, SP, Brazil

Emilio Carlos Nelli Silva

ecnsilva@usp.br

Escola Politécnica da USP

Av. Prof. Mello Moraes, 2231, 05508-030, Sao Paulo, SP, Brazil

Abstract. *An incompressible, laminar, steady state, Navier-Stokes flow problem is studied by using the Topology Optimization Method. Objective is to minimize the loss of fluid power in a unit square with one inlet and one outlet. Two approaches are used, both open source, in order to compare the methods: the first one, using the FEniCS, which uses the Finite Element Method and other, OpenFOAM, which uses the Finite Volume Method. Both methods take advantage of the adjoint methods to perform the Topology Optimization. For the FEniCS simulations, 4 different volumetric restrictions are used. It was observed that the simulation of FEniCS without volumetric restriction had results close to OpenFOAM, also without volumetric restriction. The Topology Optimization Method applied to fluids shows good potential. Although each FEM and FVM solvers have advantages and disadvantages, both have shown good tools for Topology Optimization.*

Keywords: *Fluid Topology Optimization, Computational Fluid Dynamics, Adjoint Method, Finite Volume Method, Finite Element Method.*

1 INTRODUCTION

Topology Optimization Method has been developed initially for structural problems. However, its application has been growing in field of fluids. In the method, get the sensibility of the objective function with relation to design variables is highly important to ensure good convergence in a feasible time during the optimization process. Topology Optimization of fluid flow was first introduced by Borrvall and Petersson (2003). In their pioneering work, they used a finite element approach to study a Stokes flow problem. The objective was to minimize flow dissipated power subject to volume constraint. Their work was extended by Evgrafov (2005) who included the limiting cases of pure liquid and solid. Gersborg-Hansen, Sigmund and Haber (2005) extended the applications of Topology Optimization Method to Navier Stokes flow to cover low to moderate Reynolds numbers in 2D problems. Guest and Prévost (2006) studied a variation of the method where the Stokes and Darcy equations exist as two different models, which are combined and scaled according to the permeability of each element. Othmer (2008) presented a methodology to apply the Topology Optimization Method to turbulent flows using the Finite Volume Method. This methodology is the basis for this work. A great number of other interesting works on this area can be found on literature, but for now, this discussion will limit itself to this point.

The objective of this paper is to apply the Topology Optimization Method to minimize the power loss or pressure loss of a laminar Navier-Stokes flow, *i.e.*, without a turbulence model. A unit square is given with one inlet and one outlet. The fluid path is given according to the porosity within this volume. Two approaches are used, both open source, in order to compare the methods: the first one, using the FEniCS, which uses the Finite Element Method with a point-interior optimization algorithm. The objective function of FEniCS has terms in the volumetric domain. The second one uses OpenFOAM, which uses the Finite Volume Method with a steepest descent optimization algorithm. The objective function of OpenFOAM has terms only on the surface of the domain. Both methods take advantage of the adjoint methods to perform the Topology Optimization.

This paper is organized as follows: the theoretical formulation and the adjoint method is discussed in details in section 2; the numerical implementation in OpenFOAM and FEniCS is presented on section 3; the case study used for comparisons is presented in section 4 and final remarks and conclusions are exhibited in section 5.

2 THEORETICAL FORMULATION

In a classical work, Othmer (2008) presented a methodology to apply Topology Optimization to fluid flow by using Finite Volume Method (FVM) and the Adjoint Method for the sensitivities calculation. Its theoretical formulation is presented in this session. The optimization problem is stated as follows:

$$\begin{aligned} &\textbf{Min} && J = J(\alpha, \boldsymbol{v}, p) \\ &\text{subject to:} && R(\alpha, \boldsymbol{v}, p) = 0 \end{aligned} \tag{1}$$

Proceedings of the XXXVIII Iberian Latin-American Congress on Computational Methods in Engineering
P.O. Faria, R.H. Lopez, L.F.F. Miguel, W.J.S. Gomes, M. Noronha (Editores), ABMEC, Florianópolis, SC, Brazil, November 5-8, 2017.

where J is the objective function to be maximized or minimized, $\boldsymbol{v}$ is the velocity vector, p is the pressure and α are the design variables. The restriction, $R(\alpha,\boldsymbol{v},p)=(R_1,R_2,R_3,R_4)^T$, are the Navier Stokes equations for unity density, incompressible, steady state flows (note that the strain rate tensor is represented by $D(\boldsymbol{v})=\frac{1}{2}(\nabla\boldsymbol{v}+\nabla\boldsymbol{v}^T)$).

$$(R_1,R_2,R_3)^T=(\boldsymbol{v}\cdot\nabla)\boldsymbol{v}+\nabla p-\nabla\cdot\big(2\nu D(\boldsymbol{v})\big)+\alpha\boldsymbol{v} \tag{2}$$

$$R_4=-\nabla\cdot\boldsymbol{v} \tag{3}$$

Note that R_1, R_2 and R_3 are scalars that are components that form the vector of the momentum equation, while R_4 represents an scalar of the continuity equation. Viscosity is represented by ν.

The Darcy term $\alpha\boldsymbol{v}$, which is not part of the original Navier Stokes equations, is the central component of Topology Optimization as it allows the punishment of counterproductive regions of the flow. To tackle the constrained optimization problem, the Lagrange Multipliers approach is used:

$$L=J+\int_{\Omega}(\boldsymbol{u},q)R\,d\Omega \tag{4}$$

$$(\boldsymbol{u},q)=(u_1,u_2,u_3,q) \tag{5}$$

where Ω is the flow domain, $\boldsymbol{u}$ and q are the Lagrange multipliers, conveniently named as adjoint velocity and adjoint pressure (respectively). The total variation of the Lagrangian with respect to design and state variables δL must be computed in order to find the sensitivities of the problem and is shown in Eq. (6).

$$\delta L=\delta_v L+\delta_p L+\delta_\alpha L \tag{6}$$

If Lagrange multipliers $\boldsymbol{u}$ and q are chosen such that:

$$\delta_v L+\delta_p L=0 \tag{7}$$

Sensitivities can be calculated simply from:

$$\delta L=\delta_\alpha L=\delta_\alpha J+\delta_\alpha\int_{\Omega}(\boldsymbol{u},q)R\,d\Omega=\frac{\partial J}{\partial\alpha}\delta\alpha+\frac{\partial}{\partial\alpha}\left[\int_{\Omega}(\boldsymbol{u},q)R\,d\Omega\right]\delta\alpha \tag{8}$$

By assuming no explicit dependence of the objective function on design variables, $\partial J/\partial\alpha=0$ and sensitivities can be calculated:

$$\delta_\alpha L=\int_{\Omega}\boldsymbol{u}\cdot\boldsymbol{v}\,d\Omega \tag{9}$$

Hence, for a numerical discretization, the sensitivity of cell i is the product of adjoint velocity, primal velocity and cell volume V_i:

$$\delta_\alpha L = \boldsymbol{u_i} \cdot \boldsymbol{v_i}\, V_i \tag{10}$$

2.1 Adjoint equations and boundary conditions

The Eq. (7) represents the consequence of choosing Lagrange multipliers in such a way that variation of Lagrangian with respect to velocity cancel the variation with respect to pressure. Expanding Eq. (7):

$$\delta_v J + \delta_v \int_\Omega (\boldsymbol{u}, q) R \, d\Omega + \delta_p J + \delta_p \int_\Omega (\boldsymbol{u}, q) R \, d\Omega = 0 \tag{11}$$

$$\delta_v \, (R_1, R_2, R_3)^T = (\delta v \cdot \nabla) v + (v \cdot \nabla) \delta v - \nabla \cdot \big(2 \nu D(\delta v)\big) + \alpha \delta v \tag{12}$$

$$\delta_v \, R_4 = -\nabla \cdot \delta v \tag{13}$$

$$\delta_p \, (R_1, R_2, R_3)^T = \nabla \delta p \tag{14}$$

$$\delta_p \, R_4 = 0 \tag{15}$$

Inserting Eq. (12) to (15) in Eq. (11) results:

$$\delta_v J + \delta_p J + \int_\Omega \boldsymbol{u} \cdot \Big((\delta \boldsymbol{v} \cdot \nabla) \boldsymbol{v} + (\boldsymbol{v} \cdot \nabla) \delta \boldsymbol{v} - \nabla \cdot \big(2 \nu D(\delta \boldsymbol{v})\big) + \alpha \delta \boldsymbol{v} \Big) d\Omega +$$
$$- \int_\Omega q \, \nabla \cdot \delta \boldsymbol{v} \, d\Omega + \int_\Omega \boldsymbol{u} \cdot \nabla \delta p \, d\Omega = 0 \tag{16}$$

Applying integration by parts in Eq. (16) and separating the cost function into its contributions from boundary Γ and interior Ω, Eq. (17), results in Eq. (18).

$$J = \int_\Gamma J_\Gamma \, d\Gamma + \int_\Omega J_\Omega \, d\Omega \tag{17}$$

$$\int_{\Gamma}\left(\boldsymbol{u}\cdot\boldsymbol{n}+\frac{\partial J_{\Gamma}}{\partial p}\right)\delta p\, d\Gamma+\int_{\Omega}\left(-\nabla\cdot\boldsymbol{u}+\frac{\partial J_{\Omega}}{\partial p}\right)\delta p\, d\Omega+$$

$$+\int_{\Gamma}\left(\boldsymbol{n}(\boldsymbol{u}\cdot\boldsymbol{v})+\boldsymbol{u}(\boldsymbol{v}\cdot\boldsymbol{n})+2\nu\boldsymbol{n}\cdot D(\boldsymbol{u})-q\boldsymbol{n}+\frac{\partial J_{\Gamma}}{\partial \boldsymbol{v}}\right)\cdot\delta\boldsymbol{v}\, d\Gamma+$$

$$-\int_{\Gamma}(2\nu\boldsymbol{n}\cdot D(\delta\boldsymbol{v})\cdot\boldsymbol{u})\, d\Gamma+$$

$$+\int_{\Omega}\left(-\nabla\boldsymbol{u}\cdot\boldsymbol{v}-(\boldsymbol{v}\cdot\nabla)\boldsymbol{u}-\nabla\cdot\big(2\nu D(\boldsymbol{u})\big)+\alpha\boldsymbol{u}+\nabla q+\frac{\partial J_{\Omega}}{\partial \boldsymbol{v}}\right)\cdot\delta\boldsymbol{v}\, d\Omega=0 \tag{18}$$

where $\boldsymbol{n}$ is the normal vector. In order to satisfy Eq. (18) to any $\delta\boldsymbol{v}$ and δp, the terms in parentheses must vanish. So, the integrals over the domain give rise to the adjoint Navier Stokes equations:

$$\nabla\cdot\big(2\nu D(\boldsymbol{u})\big)-\nabla q-\frac{\partial J_{\Omega}}{\partial \boldsymbol{v}}-\alpha\boldsymbol{u}=-2D(\boldsymbol{u})\boldsymbol{v} \tag{19}$$

$$\nabla\cdot\boldsymbol{u}=\frac{\partial J_{\Omega}}{\partial p} \tag{20}$$

The boundary conditions arise from the integrals over the boundaries:

$$\int_{\Gamma}\left(\boldsymbol{n}(\boldsymbol{u}\cdot\boldsymbol{v})+\boldsymbol{u}(\boldsymbol{v}\cdot\boldsymbol{n})+2\nu\boldsymbol{n}\cdot D(\boldsymbol{u})-q\boldsymbol{n}+\frac{\partial J_{\Gamma}}{\partial \boldsymbol{v}}\right)\cdot\delta\boldsymbol{v}\, d\Gamma+$$

$$-\int_{\Gamma}(2\nu\boldsymbol{n}\cdot D(\delta\boldsymbol{v})\cdot\boldsymbol{u})\, d\Gamma=0 \tag{21}$$

$$\int_{\Gamma}\left(\boldsymbol{u}\cdot\boldsymbol{n}+\frac{\partial J_{\Gamma}}{\partial p}\right)\delta p\, d\Gamma=0 \tag{22}$$

2.2 Ducted flows

In order to apply the methodology presented so far, some considerations are made to specialize it to ducted flows:

- Flow domain is considered made of three regions: inlet, wall and outlet;
- Inlet boundary conditions: prescribed velocity and zero pressure gradient;
- Wall boundary conditions: zero velocity and zero pressure gradient;
- Outlet boundary conditions: zero velocity gradient and zero pressure.

For pressure drop, it is considered that the objective function does not depend on interior of the domain, but only on integrals over the boundary surfaces. The adjoint Navier Stokes equations can be written:

$$\nabla \cdot \big(2\nu D(\boldsymbol{u})\big) - \nabla q - \alpha \boldsymbol{u} = -2D(\boldsymbol{u})\boldsymbol{v} \tag{23}$$

$$\nabla \cdot \boldsymbol{u} = \frac{\partial J_\Omega}{\partial p} \tag{24}$$

Regarding the boundary conditions, for divergenceless fields $\delta\boldsymbol{v}$ and $\boldsymbol{u}$, with at least one of them vanishing on the boundary, it can be proved that the following identity holds:

$$\begin{aligned} &\int_\Gamma 2\nu\boldsymbol{n} \cdot (D(\boldsymbol{u}) \cdot \delta\boldsymbol{v} - D(\delta\boldsymbol{v}) \cdot \boldsymbol{u})\, d\Gamma = \\ &\int_\Gamma \nu\big((\boldsymbol{n} \cdot \nabla)\boldsymbol{u} \cdot \delta\boldsymbol{v} - (\boldsymbol{n} \cdot \nabla)\delta\boldsymbol{v} \cdot \boldsymbol{u}\big)\, d\Gamma - \int_\Gamma \nabla\nu \cdot \big(\boldsymbol{u} \cdot \boldsymbol{n}\delta\boldsymbol{v} - (\delta(\boldsymbol{v} \cdot \boldsymbol{n})\boldsymbol{u})\big)\, d\Gamma \end{aligned} \tag{25}$$

It can be seen that Eq. (25) is the summing of third and sixth terms on the left side of Eq. (21). In laminar flows, ν is only the molecular viscosity, so its gradient is zero. In turbulent flows, $\nabla\nu = 0$ along the wall and also at the inlet (for homogeneously prescribed degrees of turbulence). At the outlet area, $\nabla\nu$ is generally non zero. However, the product of $\nabla\nu$ with the difference terms inside the parentheses is assumed to be second order, so this term is neglected. Therefore, Eq.(21) can be rewritten as:

$$\begin{aligned} &\int_\Gamma \left(\boldsymbol{u} \cdot \boldsymbol{n} + \frac{\partial J_\Gamma}{\partial p}\right) \delta p\, d\Gamma + \int_\Gamma \left(\boldsymbol{n}(\boldsymbol{u} \cdot \boldsymbol{v}) + \boldsymbol{u}(\boldsymbol{v} \cdot \boldsymbol{n}) + \nu(\boldsymbol{n} \cdot \nabla)\boldsymbol{u} - q\boldsymbol{n} + \frac{\partial J_\Gamma}{\partial \boldsymbol{v}}\right) \cdot \delta\boldsymbol{v}\, d\Gamma + \\ &- \int_\Gamma \nu(\boldsymbol{n} \cdot \nabla)\delta\boldsymbol{v} \cdot \boldsymbol{u}\, d\Gamma = 0 \end{aligned} \tag{26}$$

Wall and inlet. On these regions, velocity is fixed (zero on walls and prescribed value on inlet), so $\delta\boldsymbol{v} = 0$ and boundary conditions can be defined as:

$$\boldsymbol{u} \cdot \boldsymbol{n} = -\frac{\partial J_\Gamma}{\partial p} \rightarrow u_n = -\frac{\partial J_\Gamma}{\partial p} \tag{27}$$

Outlet. On this region, velocity gradient and pressure are zero, so:

$$\boldsymbol{n}(\boldsymbol{u} \cdot \boldsymbol{v}) + \boldsymbol{u}(\boldsymbol{v} \cdot \boldsymbol{n}) + \nu(\boldsymbol{n} \cdot \nabla)\boldsymbol{u} - q\boldsymbol{n} + \frac{\partial J_\Gamma}{\partial \boldsymbol{v}} = 0 \tag{28}$$

Separating Eq. (28) in its normal and tangential component:

$$\boldsymbol{u} \cdot \boldsymbol{v} + u_n v_n + \nu(\boldsymbol{n} \cdot \nabla)u_n - q + \frac{\partial J_\Gamma}{\partial v_n} = 0 \tag{29}$$

$$v_n \boldsymbol{u_t} + \nu(\boldsymbol{n} \cdot \nabla)\boldsymbol{u_t} + \frac{\partial J_\Gamma}{\partial v_t} = 0 \tag{30}$$

The normal component of the adjoint velocity on Eq. (29) can be determined by choosing an appropriate pressure field q. The tangential component of the primal velocity is used to determine the tangential component of the adjoint velocity. This set of boundary conditions completes the problem for ducted flows.

3 NUMERICAL IMPLEMENTATION

The optimization problem was solved using two different softwares: OpenFOAM (Finite Volume Method) and FEniCS (Finite Element Method). The objective was minimizing pressure drop and power loss, respectively. Details of the adjoint equations and boundary conditions related to the specific objective function are discussed in the next sections.

3.1 Topology Optimization using Open Source software - OpenFOAM

The pressure drop by a fluid dynamic device can be computed as the flux of energy through the boundaries of a control volume:

$$J = -\int_{\Gamma} \left(p + \frac{1}{2}v^2\right) \boldsymbol{v} \cdot \boldsymbol{n}\, d\Gamma \tag{31}$$

Derivatives needed for the boundary conditions are:

$$\frac{\partial J_{\Gamma}}{\partial p} = -\boldsymbol{v} \cdot \boldsymbol{n} \tag{32}$$

$$\frac{\partial J_{\Gamma}}{\partial \boldsymbol{v}} = -\left(p + \frac{1}{2}v^2\right)\boldsymbol{n} - (\boldsymbol{v} \cdot \boldsymbol{n})\boldsymbol{v} \tag{33}$$

This leads to the boundary conditions for pressure drop:

$$Inlet: \quad u_n = v_n \tag{34}$$

$$Wall: \quad u_n = 0 \tag{35}$$

$$Outlet: \quad \begin{cases} q = \boldsymbol{u} \cdot \boldsymbol{v} + u_n v_n + \nu(\boldsymbol{n} \cdot \nabla)u_n - \frac{1}{2}v^2 - v_n^2 \\ \quad 0 = v_n(\boldsymbol{u_t} - \boldsymbol{v_t}) + \nu(\boldsymbol{n} \cdot \nabla)\boldsymbol{u_t} \end{cases} \tag{36}$$

The solver used in OpenFOAM is available in the default package under the name of `adjointShapeOptimizationFoam`. In this work, the flow is modeled as a laminar newtonian fluid. Optimization is applied to ducted shape geometries by "blocking" regions causing pressure loss as estimated using an adjoint formulation (Greenshields, 2017).

The default implementation of the solver optimizes for total pressure loss, although the methodology exhibited in the original paper by Othmer (2008) describes the method for optimizing power loss and flow uniformity. In this paper, the power loss was implemented.

Optimization is performed by an implementation of steepest descent method.

Primal equations are solved using the Semi Implicit Pressure Linked Equations (SIMPLE) algorithm. Adjoint equations are solved using a similar approach (Othmer, de Villiers, Weller, 2007).

3.2 Topology Optimization using FEniCS

The FEniCS Project consists in a collection of components and libraries for numerical simulation, automating the solution of Partial Differential Equations (PDEs) by the Finite Element Method (FEM). It is a high-level programming software that able to interpret a system of equations in a variational form using the Python language. The implementation of the relevant transport equations in FEniCS gives direct access to any requested information, besides greater knowledge of its numerical implementation.

Rewriting Eq.(2) and Eq.(3), the continuity and the incompressible Navier-Stokes equations, without considering the gravity, results in the Eq.(37) and Eq.(38).

$$\nabla \cdot \boldsymbol{v} = 0 \tag{37}$$

$$\boldsymbol{v} \cdot \nabla \boldsymbol{v} = -\nabla p + \mu \nabla^2 \boldsymbol{v} - \alpha \boldsymbol{v} \tag{38}$$

The variational form of these equations are given by multiplying for test functions and integrating in the domain Ω, resulting in the following equations bellow.

$$\int_\Omega (\nabla \cdot \boldsymbol{v}) q dx = 0 \tag{39}$$

$$\int_\Omega (\boldsymbol{v} \cdot \nabla \boldsymbol{v}) \ \cdot \boldsymbol{u} dx = + \int_\Omega p \nabla \cdot \boldsymbol{u} \, dx - \mu \int_\Omega \nabla \boldsymbol{v} : \nabla \boldsymbol{u} \, dx - \int_\Omega \alpha (\boldsymbol{v} \cdot \boldsymbol{u}) dx \tag{40}$$

where q and $\boldsymbol{u}$ are test function. Using $\langle , \rangle$ as the inner product, resulting in the following weak-form equations.

$$\langle \nabla \cdot \boldsymbol{v}, q \rangle = 0 \tag{41}$$

$$\langle \boldsymbol{v} \cdot \nabla \boldsymbol{v}, \boldsymbol{u} \rangle = \langle p, \nabla \cdot \boldsymbol{v} \rangle - \mu \langle \nabla \boldsymbol{v}, \nabla \boldsymbol{u} \rangle - \alpha \langle \boldsymbol{v}, \boldsymbol{u} \rangle \tag{42}$$

The porosity value is given by a value within the range $[\underline{\alpha}; \overline{\alpha}]$. For the determination of the low or high porosity α, it is desired to have a function which relates the minimum and maximum values of α by a range of pseudo-density ρ 0.0 to 1.0. Thus, a null pseudo-density results in $\underline{\alpha}$ and pseudo-density 1.0, resulting in $\overline{\alpha}$. It wants a function that results in values close to one of the extremes, otherwise it could result in intermediate porosity values, which is surreal when the presence of material in the region is desired or not. Furthermore, a linear function imposes an excessive constraint, which can converge to a locally optimized solution. Thus, Borrvall and Petersson (2003) suggest a convex and q-parameterized interpolation function, shown in Eq. (43).

$$\alpha(\rho) = \overline{\alpha} + (\underline{\alpha} - \overline{\alpha}) \rho \, \frac{1 + q}{\rho + q} \tag{43}$$

The parameter $q > 0$ is a penalty used. The smaller, more convex the function α. An example, with four different values of q, is shown Figure 1. Also, the figure shows the $\underline{\alpha} = 2.5\mu/100^2$ and $\overline{\alpha} = 2.5\mu/0.01^2$, used in the FEniCS simulations. As can be seen, the lower the value of q, the lower the intermediate values of α.

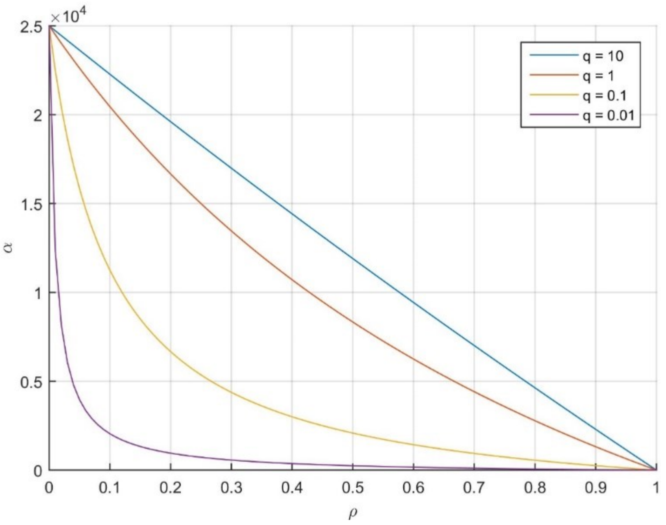

Figure 1 - Material Function Interpolation for 4 values of q

The IPOpt is used as the interior-point optimization software. It uses a primal-dual barrier method that solves a sequence of barrier problems. More information about IPOpt can be found in Wächter (2009).

4 CASE STUDY

The case studied is based on the pipe bend example showed by Borrvall and Petersson (2003). Objective is to find the flow path with the least energy dissipation. Design domain is unit square. Inlet and Outlet are 0.1 length and are located 0.1 distant from the closest edge. The geometry can be seen in Figure 2.

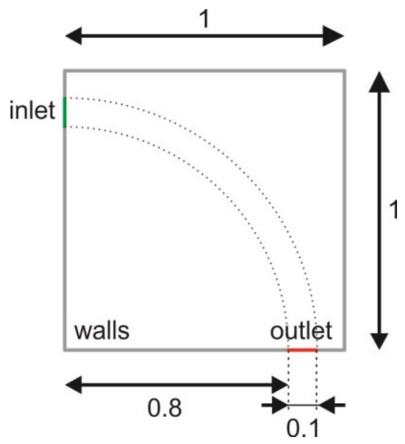

Figure 2. Design domain

The meshes used were different among the simulations, since these are different methods (FVM and FEM) for the solution of fluid equations. Figure 3 shows the comparison between meshes. The number of elements of the FEniCS is smaller when compared to the one used in OpenFOAM, because it is a FEM solver. Also, the FEniCS elements are triangular, against the OpenFOAM's quadrilaterals.

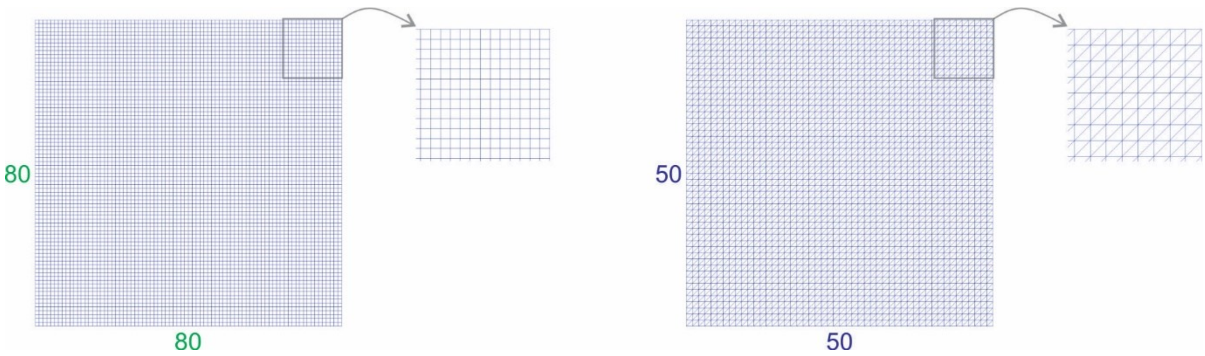

Figure 3 - Mesh compare between OpenFOAM (left) and FEniCS (right)

Both simulations in OpenFOAM and FEniCS follow the same optimization loop scheme, shown in Figure 4, which shows what each simulation uses in each step of the process in green text (for OpenFOAM) or blue text (for FEniCS).

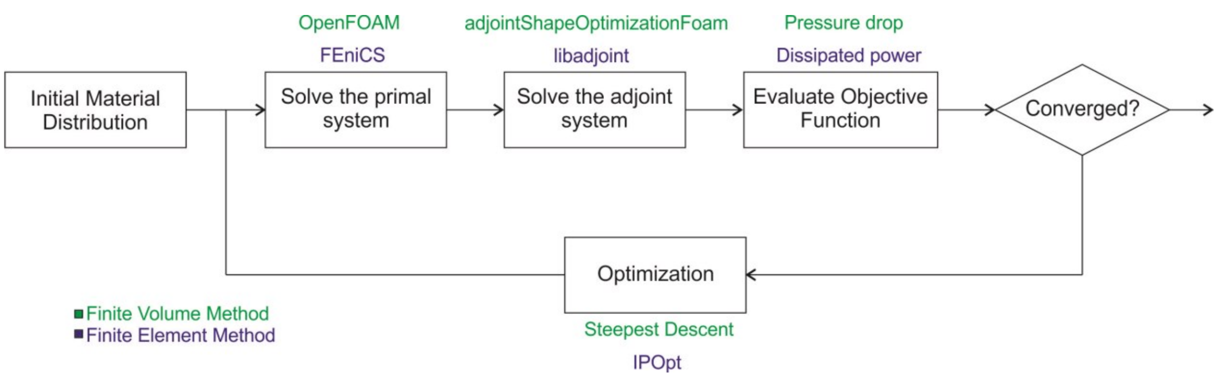

Figure 4 - Optimization Loop

4.1 OpenFOAM

For the simulation in OpenFOAM, the formulation of the optimization problem is described below.

$$\begin{array}{ll} \underset{\alpha}{\textbf{Min}} & J = \int_{\Gamma} d\Gamma \left(p + \frac{1}{2}v^2\right) \boldsymbol{v} \cdot \boldsymbol{n} \\ \text{subject to:} & \text{Eq(2)} \\ & \text{Eq(3)} \\ & 0 \leq \alpha \leq 200 \end{array}$$

The contour conditions in the inlet are velocity of 2.5 m/s and zero pressure gradient. In the outlet, zero velocity gradient and zero pressure. The viscosity is $\nu = 0.01$. Minimum and maximum of α are 0 and 200 respectively. The boundary conditions `adjointOutletVelocity` and `adjointOutletPressure` were implemented and deal with boundary conditions like the description showed in section 3.1. Optimization was set up to run for 3000 iterations, when the problem was considered converged. The results are shown in Figure 5.

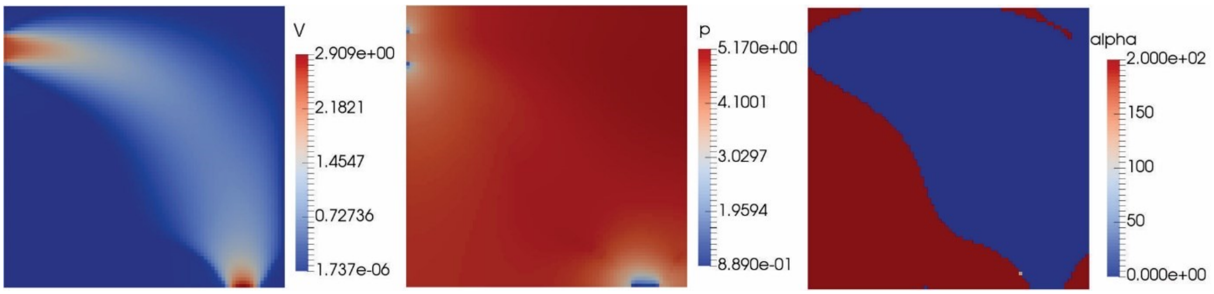

Figure 5 - OpenFOAM optimization result

4.2 FEniCS

For the simulation in FEniCS, the formulation of the optimization problem is described below.

$$\begin{array}{ll} \underset{\rho}{\textbf{Min}} & J = \frac{1}{2}\int_{\Omega} \alpha(\rho)\boldsymbol{v} \cdot \boldsymbol{v} + \frac{\mu}{2}\int_{\Omega} \nabla\boldsymbol{v} : \nabla\boldsymbol{v} \\ \text{subject to:} & \text{Eq. (41)} \\ & \text{Eq. (42)} \\ & 0 \leq \rho \leq 1 \\ & \int_{\Omega} \rho \leq V_{max} \end{array}$$

The contour conditions in the inlet and the outlet are the velocity of 2.5 m/s and zero pressure gradient. The viscosity is $\mu = 0.01$ and the q from material function interpolation is $q = 0.01$. Taylor-Hood function is used; with the vector element of velocity has polynomial element degree of 2; and pressure scalar element, polynomial element degree of 1.

Simulations were performed with 4 different volume restrictions (V_{max}), in which the last one being without restriction. The results are shown in the following figures.

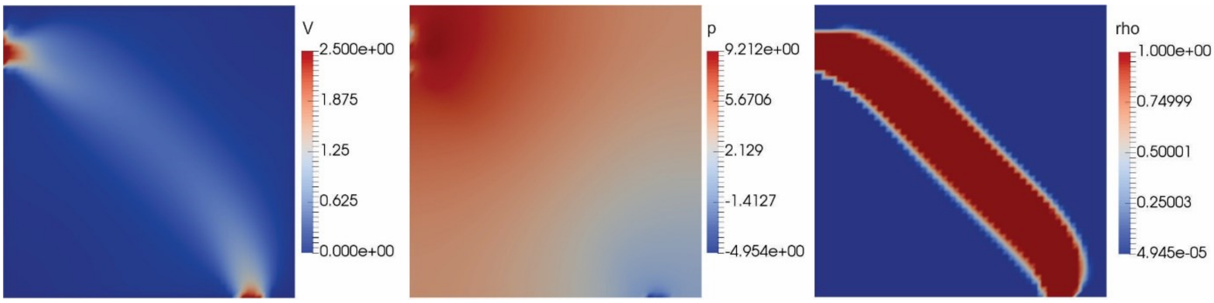

Figure 6 - FEniCS optimization result with $V_{max} \leq 0.25$

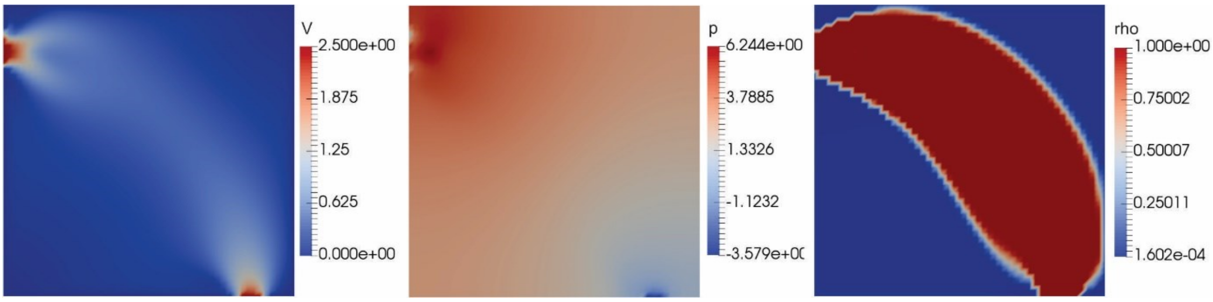

Figure 7 - FEniCS optimization result with $V_{max} \leq 0.5$

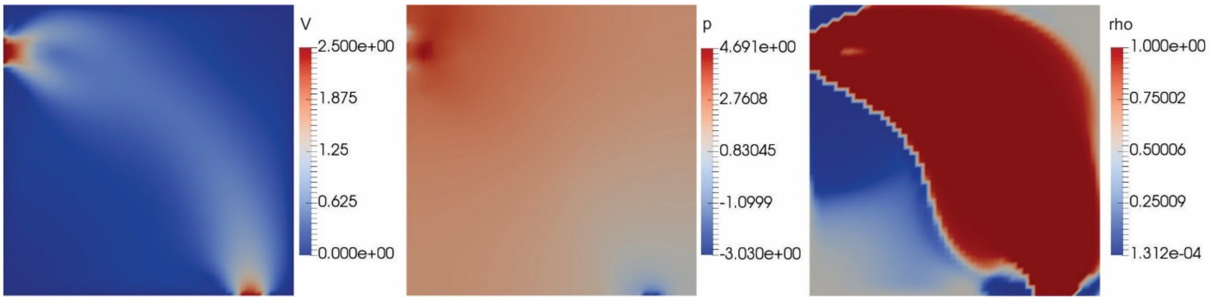

Figure 8 - FEniCS optimization result with $V_{max} \leq 0.75$

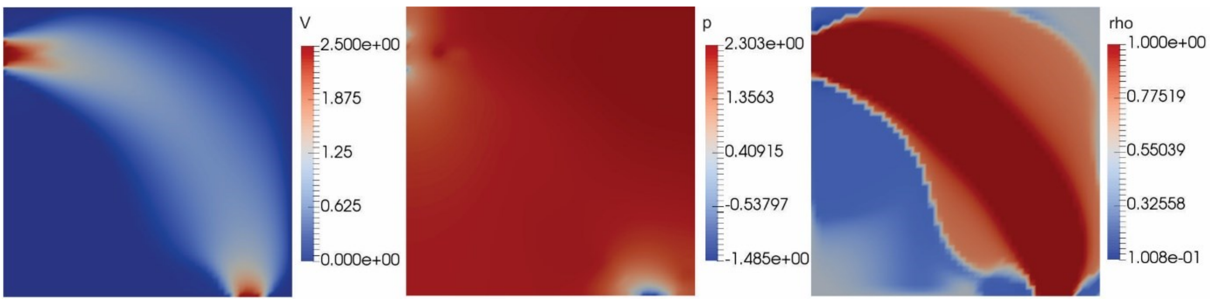

Figure 9- FEniCS optimization result without volume restriction

5 FINAL REMARKS AND CONCLUSIONS

It is observed that, for the unrestricted case of volume using FEniCS, its result approached considerably the Topology Optimization obtained by OpenFOAM, showing that the objective functions are equivalent, finding the same distribution of porosity, besides the two methods bring satisfactory results.

The Topology Optimization Method applied to fluids shows good potential. Although each FEM and FVM solvers have advantages and disadvantages, both have shown good tools for Topology Optimization. Two open source software were used, which allows to investigate and change the current code.

Future steps are planned for both FEniCS and OpenFOAM platform. In OpenFOAM, it is intended to apply the material penalty method, as it was used in FEniCS, avoiding possible green zones. Also, it is intended to perform simulations with volumetric restrictions, allowing a direct comparison with the FEniCS results. Although not presented in this paper, the use of turbulence model has already been implemented in OpenFOAM, having difficulty to implement a wall treatment model. The optimization algorithm used in OpenFOAM (steepest descent) can be improved for a more robust and efficient algorithm, such as the IPOpt, used in the Topology Optimization in FEniCS. The next step using FEniCS is to include a turbulence model.

ACKNOWLEDGEMENTS

The authors gratefully acknowledge support from BG/Shell Brasil and FAPESP through the Research Centre for Gas Innovation - RCGI (Fapesp Proc.2014/50279-4), hosted at the University of Sao Paulo, and the strategic importance of the support given by ANP (Brazil's National Oil, Natural Gas and Biofuels Agency) through the R&D regulation. The authors also acknowledge the CNPq (National Council for Research and Development) process 304121/2013-4 for financial support.

REFERENCES

Borrvall, T., Petersson, J., 2003. Topology optimization of fluids in Stokes flow. *International Journal for Numerical Methods in Fluids*, vol. 41, pp. 77–107.

Evgrafov, A., 2005. The Limits of Porous Materials in the Topology Optimization of Stokes Flows. *Applied Mathematics & Optimization*, vol. 52, pp. 263-277.

Gersborg-Hansen, A., Sigmund, O., Haber, R. B., 2005. Topology optimization of channel flow problems. *Structural Multidisciplinary Optimization*, v. 90, pp. 90-120.

Greenshields, C. J., 2017. *OpenFOAM User Guide Version 5.0,* OpenFOAM Foundation Ltd.

Guest, J. K., Prévost, J. H., 2006. Topology optimization of creeping fluid flows using a Darcy-Stokes finite element. *International Journal for Numerical Methods In Engineering*, v. 66, pp. 461-484.

Othmer, C., 2008. A continuous adjoint formulation for the computation of topological and surface sensitivities of ducted flows. *International Journal for Numerical Methods in Fluids*, vol. 58, pp. 861–877.

Othmer, C., de Villiers, E., & Weller, H. G., 2007. Implementation of a continuous adjoint for topology optimization of ducted flows. In *18th AIAA Computational Fluid Dynamics Conference*, pp. 1–7.

Wächter, Andreas., 2009. *Short tutorial: getting started with ipopt in 90 minutes*. In: Dagstuhl Seminar Proceedings. Schloss Dagstuhl-Leibniz-Zentrum für Informatik.